E-proceedings of the 38th IAHR World Congress
September 1-6, 2019, Panama City, Panama
doi:10.3850/38WC092019-1595

A Moving Particle Semi-implicit numerical method for modelling sediment dynamic

MOJTABA JANDAGHIAN[(1)], AHMAD SHAKIBAEINIA[(1)]

[(1)]Department of Civil, Geological and Mining Engineering, Polytechnique Montréal, Montréal, Canada
mojtaba.jandaghian@polymtl.ca; ahmad.shakibaeinia@polymtl.ca

ABSTRACT

Fluvial/coastal sediment transport, debris flows, and landslides are a few examples of sediment dynamic problems. Modelling and predicting the mechanical behaviours of these so-called multiphase granular flows are crucial for optimum engineering designs and hazard management. The mesh-free particle approaches, with an inherent ability to deal with highly-dynamic multiphase systems, are becoming the powerful tools for such predictions. This research paper aims to develop and evaluate an improved mesh-free particle model, based on a multiphase Weakly Compressible Moving Particle Semi-implicit (WC-MPS) method to model a gravity-driven sediment dynamic problem in subaerial and subaquatic conditions. Several stability improvement techniques are adapted to WC-MPS model to overcome the tensile instability and the noisy pressure fields that may affect sediment behaviour. These include an optimized particle shifting approach and a new numerical diffusion term. A visco-plastic rheological model based on local $\mu(I)$ rheology is used to predict the non-Newtonian behaviour of sediment continuum. The collapse of granular materials (a widely-used test case) is used as the benchmark of this study. The surface profiles and the runout distance of the granular deposits are compared and evaluated with those of the experimental measurements showing good compatibility. The implemented and adapted improvement techniques are proven to be effective in reproducing realistic sediment behaviours in different flow conditions.

Keywords: Sediment dynamic; multiphase granular continuum; WC-MPS method; meshfree Lagrangian modelling; the $\mu(I)$ rheology.

1 INTRODUCTION

While the mesh-based Eulerian numerical methods have been proven to be effective for some sediment dynamic problems, dealing with the highly dynamic movement of sediment/granular material is beyond their capabilities. Mesh-free particle methods have the flexibility to model complex deformations and fragmentation, so they provide a unique opportunity for modelling of multiphase granular flow problems. Smoothed Particles Hydrodynamics (SPH) and Moving Particles Semi-implicit (MPS) approaches are well developed mesh-free particles models employed in continuum modelling of Newtonian and non-Newtonian fluid flows (e.g. Khanpour et al., 2016; Shakibaeinia and Jin, 2011). Since the continuum models simulate a bulk volume of material, they are computationally affordable in comparison to the discrete Lagrangian approaches such as Discrete Element Method (DEM). Koshizuka and Oka (1996) proposed the MPS method for simulating incompressible fluid flows. Shakibaeinia and Jin (2010) utilized the equation of state for calculating the pressure term as a function of the particle number density instead of solving Poisson's pressure equation. The equation of state makes the fluid flow weakly compressible with respect to the Mach number set to less than 0.1.

The rheological models as the constitutive laws consider the granular materials as non-Newtonian fluids. Since the rheological models are largely dependent on the yield stress as a function of the pressure field, they are sensitive to any instabilities and unphysical fluctuations (vibration) in the pressure field. Moreover, the mesh-free particle models suffer from the particle interpenetration so-called tensile instability due to the insufficient repulsive force between particles. Lind et al. (2012) proposed the particle shifting algorithm to disposition particle to the area with less particle concentration according to the Fick's law of diffusion and Khayyer et al. (2017) optimized the particle shifting toward the free surface via detecting the free surface layer and modifying the shifting vector. Molteni and Colagrossi (2009) inserted a diffusion term into the continuity equation as a pure numerical correction method in the weakly compressible SPH model to improve the pressure evaluation.

In this paper, we employ our developed WC-MPS model to simulate the granular collapse as the flow of a continuum material in which we reproduce the behaviour of the granular phase using a visco-plastic constitutive law called the local $\mu(I)$ rheology (See Jop et al., 2006). To overcome the instabilities associated with the MPS method, we implement the optimized particle shifting approach to regularize particle distribution and append a diffusion term into the divergence-free model to eliminate the noisy pressure field. We consider the collapse of the dry and submerged granular material as two-dimensional problems and compare the extracted surface

profiles and the runout distances with the experimental results. Moreover, we evaluate and discuss the role of the enhancement methods in eliminating the tensile instability and consequent improvement in sediment behaviour.

2 METHODOLOGY

2.1 Weakly Compressible MPS basics

To model the multiphase granular material as a continuum phase via the MPS method, the representative volume of sediment mixture is homogenized into moving particles carrying the material and flow properties (The position, $\mathbf{x}_i$, velocity, $\mathbf{v}_i$, pressure, p_i, density, ρ_i, dynamic viscosity, μ_i, and particle number density, n_i, of particle i). The volume fraction of the granular phase (ϕ_g) and the water porosity ($1-\phi_g$) determine the density of the particles. (Figure 1)

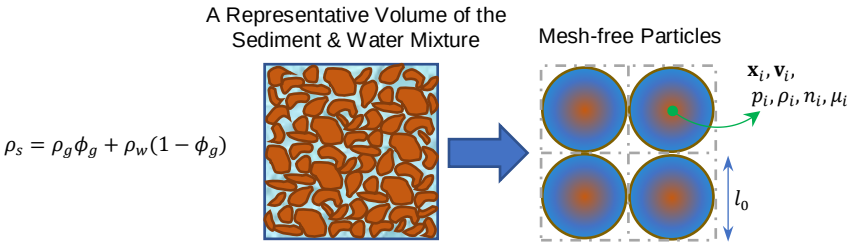

Figure 1. Homogenization of the representative volume of the mixture into moving particles

As the threshold and shear rate dependency exists in the sediment flow behaviours, we treat the granular material as a non-Newtonian fluid through the Navier-Stokes equations and the rheological models (i.e. the constitutive equations) (Jop et al., 2006). The continuity and momentum equations in the Lagrangian framework are as follow:

$$\frac{D\rho_i}{Dt} + \rho_i \nabla . \mathbf{v}_i = 0 \quad [1]$$

$$\rho_i \frac{D\mathbf{v}_i}{Dt} = -\nabla . \mathbf{T}_i + \mathbf{F}_i \quad [2]$$

where $\mathbf{F}_i$ is the body forces vector acting on particle i. The general form of the total stress tensor, $\mathbf{T}_i$, is the sum of the thermodynamic pressure (p_i) and the viscous shear stress tensor ($\boldsymbol{\tau}_i$), i.e.:

$$\mathbf{T}_i = -p_i\mathbf{I} + \boldsymbol{\tau}_i(\mathbf{E}_i) \quad [3]$$

in which $\mathbf{I}$ is the identity matrix and $\mathbf{E}_i$, the strain rate tensor, represents the rate of deformation for the incompressible fluid flows as:

$$\mathbf{E}_i = \frac{1}{2}(\nabla\mathbf{v}_i + \nabla\mathbf{v}_i^T) \quad [4]$$

For the incompressible Newtonian fluid flows where $\nabla . \mathbf{v}_i = 0$ and the linear relation between the strain rate and shear stress exists the divergence of the viscous shear stress is rewritten as:

$$\nabla . \boldsymbol{\tau}_i = \mu_i \nabla^2 \mathbf{v}_i \quad [5]$$

By calculating the effective dynamic viscosity ($\mu_{eff.}$) with the constitutive models, the WC-MPS model employs Eq. [5] to implement the divergence of shear stress of the non-Newtonian fluid in the momentum equation. The equation of state in the context of MPS updates the pressure field by the particle number density from the continuity equation as (Shakibaeinia and Jin, 2010):

$$p_i = \frac{c_0^2\rho_0}{\gamma}\left(\left(\frac{n_i}{n_0}\right)^\gamma - 1\right), \gamma = 7 \quad [6]$$

where n_0 is the maximum particle number density of particles at the initial time step and c_0 is the reference sound speed equal to $10V_{max}$ limiting the compressibility to 1 % (V_{max}: the maximum velocity magnitude).

In the MPS method to estimate a flow variable for a moving particle i, the particle approximation procedure smooths variables of the neighbor particles with a weighting function so-called the kernel function (W). If the distance between particle i and j, $r_{ij} = |r_j - r_i|$, is less than the smoothing length of the kernel function, r_e, we label particle j as the neighbour particle of particle i. Here, the smoothing length is set to 3.1 of the initial distance of the particles, l_0 and the third-order polynomial spiky function proposed by Shakibaeinia and Jin (2010) is employed for the particle approximation:

$$W(r_{ij}, r_e) = \begin{cases} (1-q)^3, & 0 \le q < 1 \\ 0, & 1 \le q = \dfrac{r_{ij}}{r_e} \end{cases} \quad [7]$$

The kernel summation equation calculates the maximum particle number density at $t = 0$ (i.e. $n_0 = \max(\sum_{i \neq j}^{n} W_{ij}(r_{ij}, r_e))$). The divergence of velocity and the pressure gradient are approximated via the MPS formulations as (Koshizuka et al., 2018):

$$\langle \nabla . \mathbf{v} \rangle_i = \frac{d}{n_0} \sum_{i \neq j}^{n} \frac{\mathbf{v}_j - \mathbf{v}_i}{r_{ij}} . \mathbf{e}_{ij} W_{ij} \quad [8]$$

$$\langle \nabla p \rangle_i = \frac{d}{n_0} \sum_{i \neq j}^{n} \frac{p_j + p_i}{r_{ij}} \mathbf{e}_{ij} W_{ij} \quad [9]$$

in which d is the dimension of the problem (here, $d = 2$) and $\mathbf{e}_{ij} = \frac{\mathbf{r}_{ij}}{|r_{ij}|}$. The Laplacian of the velocity vector considering the harmonic mean of dynamic viscosity of particles i and j is formulated as follow (Shakibaeinia and Jin, 2011):

$$\langle \nabla(\mu_i \nabla . \mathbf{v}) \rangle_i = \frac{4d}{\lambda n_0} \sum_{i \neq j}^{n} \frac{\mu_i \mu_j}{\mu_i + \mu_j} \frac{\mathbf{v}_j - \mathbf{v}_i}{r_{ij}} W_{ij} \quad [10]$$

We employ the second order Symplectic time integration algorithm (Monaghan and Rafiee, 2013) to solve the governing equations explicitly by limiting the time steps (Δt) based on the Courant–Friedrichs–Lewy stability condition (CFL condition) by $\Delta t \le CFL \frac{l_0}{c_0}$. It should be noted that by setting the CFL coefficient equal to 0.05 we will satisfy the maximum force and viscosity conditions in determining the time steps of the calculation.

2.2 The local- $\mu(I)$ rheology

Jop et al. (2006) and Forterre and Pouliquen (2008) proposed a constitutive model specific for the granular flows by employing dimensionless parameters to define the threshold and the shear stress of the flow (i.e. the effective viscosity). A simple plane shear configuration in the absence of gravity explains the structure of the dense granular flows with the dimensionless parameters; the friction coefficient, μ, and the inertial parameter, I. The inertial number, I, as a ratio of the microscopic time scale, t_{micro}, to the macroscopic timescale, $t_{macro} = 1/\|\mathbf{E}\|$, specifies the granular flow regimes where small values of I stand for the quasi-static regimes with less kinetic energy, while large values of I correspond to rapid flows (Jop, 2015).

For the dry and dense granular flows (the free fall regime) and the submerged granular collapse (the inertial regime), the inertial numbers are given as:

$$I = \begin{cases} \dfrac{\|\mathbf{E}\| d_g}{\sqrt{p_m/\rho_s}} \rightarrow \text{Free fall regime} \\ \dfrac{\|\mathbf{E}\| d_g}{\sqrt{p_m/\rho_w C_d}} \rightarrow \text{Inertial regime} \end{cases} \quad [11]$$

in which $\|\mathbf{E}\|$ is the square of the second main invariant of $\mathbf{E}$ (i.e. $\|\mathbf{E}\| = \sqrt{II_E}$), ρ_s = the solid grains density, ρ_w = the water density, C_d =the drag coefficient and p_m = the mechanical pressure between grains (i.e. the effective normal stress within the solid phase). With the dimensional analysis expressing only two dimensionless parameters for the plane shear problem, the friction coefficient (μ) and the volume fraction (ϕ_g) would be only functions of I (I from 0.01 to 0.5) (Jop, 2015). Hence, the constitutive law represents the shear stress as a function of the friction, the normal stress and the volume fraction by $\boldsymbol{\tau}(\mathbf{E}) = \mu(I) p_m$ and $\phi_g = \phi(I)$. By evaluating the experimental results and numerical simulations, the local friction and volume fraction laws are expressed analytically as (Jop et al., 2006):

$$\mu(I) = \mu_s + \frac{\tan\theta_{\mu 2} - \tan\theta_{\mu s}}{I_0/I + 1}, \qquad \phi(I) = \phi_{max} + (\phi_{min} - \phi_{max})I \quad [12]$$

in which I_0 is a material dependent constant, $\theta_{\mu s}$ and $\theta_{\mu 2}$ are the lower and upper limits of the friction angles and ϕ_{max} and ϕ_{min} are the maximum and minimum volume fractions related the granular material properties. Since the dense granular flow (i.e. the liquid regime) is considered as an incompressible non-Newtonian fluid, the local rheological model calculates the effective viscosity by $\mu_{eff} = \mu(I)p_m/2\|\mathbf{E}\|$. To avoid singularity when $\|\mathbf{E}\| \to 0$, we employ the Herschel-Bulkley-Papanastasiou (HBP) model to represent the effective viscosity with:

$$\mu_{eff} = \frac{\mu_s p_m(1 - \exp(-m\|\mathbf{E}\|))}{2\|\mathbf{E}\|} + \mu_0(2\|\mathbf{E}\|)^{N-1} \quad [13]$$

where m and N are the exponential growth controller and the power-law coefficients, respectively (Zubeldia et al., 2018) and $\mu_0 = \left(\frac{\tan\theta_{\mu 2} - \tan\theta_{\mu s}}{\frac{I_0}{I}+1}\right)\frac{p_m}{2\|\mathbf{E}\|}$ from Eq. [12]. We should note that the μ(I) rheology considers a variable expression for the coefficient of the post-failure term (the second term in the RHS of Eq. [13]) as a function of the mechanical pressure and the material properties (Tajnesaie et al., 2018). We employ the Drucker-Prager model with $\alpha = \frac{2\sqrt{3}\sin\theta_{\mu s}}{3-\sin\theta_{\mu s}}$ to calculate the yield stress through $\tau_y = \alpha p_m$ similar to the work of Zubeldia et al. (2018) for the non-cohesive granular material. Eq. [13] limits the maximum effective viscosity as $\|\mathbf{E}\| \to 0$ to $0.5m\tau_y + \mu_0$ (where $N = 1$). Also, the model calculates the effective pressure within the solid grains (i.e. p_{eff} for the submerged case) by subtracting the hydrostatic water pressure at the sediment particle from the smoothed bulk pressure obtained via the equation of state.

2.3 A diffusion term in the context of WC-MPS

In the SPH method, Molteni and Colagrossi (2009) as a pure numerical correction approach similar to the role of the artificial term of Monaghan (1992) added a diffusive term to the right hand side of the continuity equation to reduce the approximation errors and the noise in the pressure field. Similarly, we derive a new diffusive term in the WC-MPS framework using the standard form of the pressure gradient, the continuity equation and the equation of state as follows:

$$D_i = \delta\frac{\Delta t c_0^2}{n_0}\nabla^2 n_i \quad [14]$$

in which the non-dimensional coefficient, δ, $(0 < \delta \leq 1)$ determines the strength of the diffusive term and Δt is the time step size. Eventually, the continuity equation forms to the following equation by implementing the diffusion term and considering the relation between the density and the particle number density of particle i as:

$$\frac{1}{n_i}\frac{Dn_i}{Dt} = -\nabla.\,\mathbf{v}_i + \delta\frac{\Delta t c_0^2}{n_0}\nabla^2 n_i \quad [15]$$

In our WC-MPS model, Eq. [15] updates the particle number density of the particles (n_i) in each time step based on the velocity field of that time step and the Laplacian of n_i of the previous time step.

2.4 Optimized Particle Shifting Algorithm

Eliminating the tensile instability requires the model to utilize enhancement techniques to reposition particles based on the Fick's law of diffusion or by adding an artificial repulsive force to the momentum equation. Here, we supply our WC-MPS model with the optimized particle shifting algorithm proposed by Lind et al. (2012). In the MPS framework, to regularize the particle distribution, we disposition particles with respect to the particle concentration defined as:

$$C_i = \frac{\sum_{i\neq j}^{n} W_{ij}}{n_0} \quad [16]$$

Akin to the pressure gradient term (Eq. [9]), we propose an antisymmetric form of the gradient of particle concentration as:

$$\langle \nabla C_i \rangle = \frac{d}{n_0} \sum_{i \neq j}^{n} \frac{C_i + C_j}{r_{ij}} \mathbf{e}_{ij} W_{ij} \qquad [17]$$

by which the particle shifting vector lies on $\mathbf{r}_{ij}$ and has the conservation feature of the shifting procedure. Moreover, Eq. [17] without the gradient of kernel function is independent of the artificial repulsive force Lind et al. (2012) inserted into the particle shifting equation to eliminate the possible tensile instability. Based on the implemented particle classification scheme (i.e. distinguishing the free surface particles ($i \in \mathbb{F}$) from internal ($i \in \mathbb{I}$) and external particles ($i \in \mathbb{E}$)), the optimized particle shifting approach proposed by Khayyer et al. (2017) corrects the shifting vector of particle i as:

$$\delta \mathbf{r}_i = \begin{cases} -F_i \nabla C_i, & \text{if } i \in \mathbb{I} \\ -F_i (\boldsymbol{I} - \mathbf{n}_i \otimes \mathbf{n}_i).\nabla C_i\,, & \text{if } i \in \mathbb{F} \\ 0 & \text{if } i \in \mathbb{E} \end{cases} \qquad [18]$$

in which $\boldsymbol{I}$ is the identity matrix, $\mathbf{n}_i$ is the normal vector to the free surface calculated similar to the work of Duan et al. (2018) as:

$$\mathbf{n}_i = -\frac{\mathbf{N}_i}{\|\mathbf{N}_i\|}, \qquad \mathbf{N}_i = \sum_{i \in \mathbb{F}, i \neq j}^{n} \mathbf{e}_{ij} W_{ij} \qquad [19]$$

and F_i is the Fickian diffusion coefficient. According to the maximum velocity, the particles distances and the time steps, the model calculates the Fickian diffusion coefficient for the particle shifting algorithm with $F_i = 0.5 l_0 \Delta t V_{max}$.

3 RESULTS AND DISCUSSIONS

The initial setup of the experimental and numerical models for the subaerial and subaquatic problems are illustrated in Figure 2. In these test cases the gravitational acceleration in the y direction, $\mathbf{g} = (0, -9.81\ m/s^2)$, collapses the granular material as the gate moves up with a constant velocity of $V_g = 2\ m/s$. Table 1 contains the problems specifications and material properties of the sediment and water phases. The friction angles ($\theta_{\mu 2}$, $\theta_{\mu s}$), the grains density (ρ_g) and the volume fractions (ϕ_{min}, ϕ_{max}) of the sediment phase correspond to the glass beads with the mean diameter, $d_g = 0.0008\ m$ and $I_0 = 0.279$. We position the mesh-free particles on a cartesian lattice with the initial particle distance, l_0 = 0.001 and 0.002 m to simulate the subaerial and subaquatic cases via our developed continuum WC-MPS model. The initial pressure field is assigned to the particles according to their position and material density in the static condition. The exponential and power-law coefficients of the Herschel-Bulkley model (Eq. [13]) are adjusted by sensitivity analysis with respect to the experimental results. Also, the solid walls are simulated via the fixed ghost particles to complete the kernel support of the moving particles closed to the boundaries.

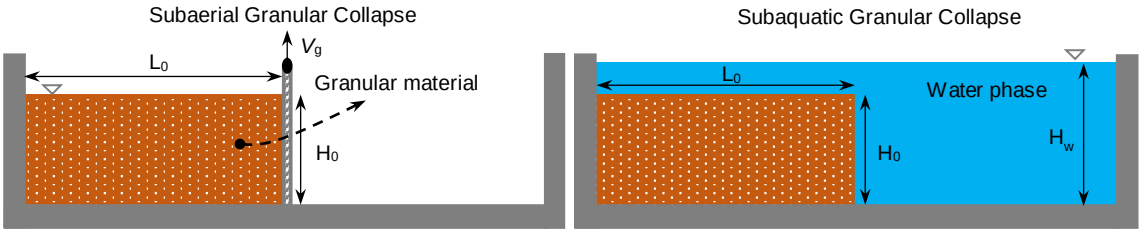

Figure 2. The granular collapse initial setups; the subaerial (Left) and subaquatic (Right) configurations

Table 1. The subaerial and subaquatic problems specifications and material properties

Setup	H_0 (m)	L_0 (m)	H_W (m)	c_0 (m/s)	ρ_w (kg/m^3)	μ_w Pa. s	ρ_g (kg/m^3)	ρ_s (kg/m^3)	C_d	ϕ_{min}, ϕ_{max}	d_g (m)	I_0	m, N	$\theta_{\mu 2}$, $\theta_{\mu s}$ (degree)
Subaerial	0.049	0.0975	---	10	---	---	2500	1536	---	0.63, 0.58	0.0008	0.279	50, 0.7	35, 22
Subaquatic	0.048	0.0975	0.07	10	1000	0.001	2500	1945	0.47	0.63, 0.58	0.0008	0.279	50, 0.7	35, 22

3.1 Subaerial granular collapse

To simulate the granular material collapse with aspect ration 0.5, we set the calculation time steps to 5×10^{-6} and 1×10^{-5} second for $l_0 = 0.001$ and 0.002 m configurations satisfying the CFL and maximum viscosity conditions. The particle number density for updating the pressure field is calculated in each time step via the

continuity equation with $\delta = 0.2$ for the proposed diffusive term. The local *μ(I)* rheology by considering the dry granular flow as the free fall regime includes the shear stresses via Eq. [10] in the momentum equation.

We compare the time evolution of the dry granular collapse with the experimental surface profiles in Figure 3B at $t = 0.08, 0.25$ and 0.50 second (The green and red colours are only set to better illustrate the deformation). The surface profiles extracted from the experiments (Figure 3A and the black squares in Figure 3B) are plotted on the simulation outputs showing relatively good agreements among the numerical model and experiments. The viscosity ($\log \mu_{eff}$) and the total velocity (V) fields in Figure 3C & D illustrate the yielded (failure) and non-yielded zones. The region with zero velocity as a trapezoidal shape zone forms since the granular material starts to collapse at $t = 0.08\ sec$.. The yielded region decreases as time goes on, while the frontier face avalanches on the bed wall and finally stops with the viscosity reaching its maximum value and $V = 0$ at $t = 0.5\ sec$. The mechanical pressure field calculated by the equation of state (Eq. [6]) is represented in Figure 3E.

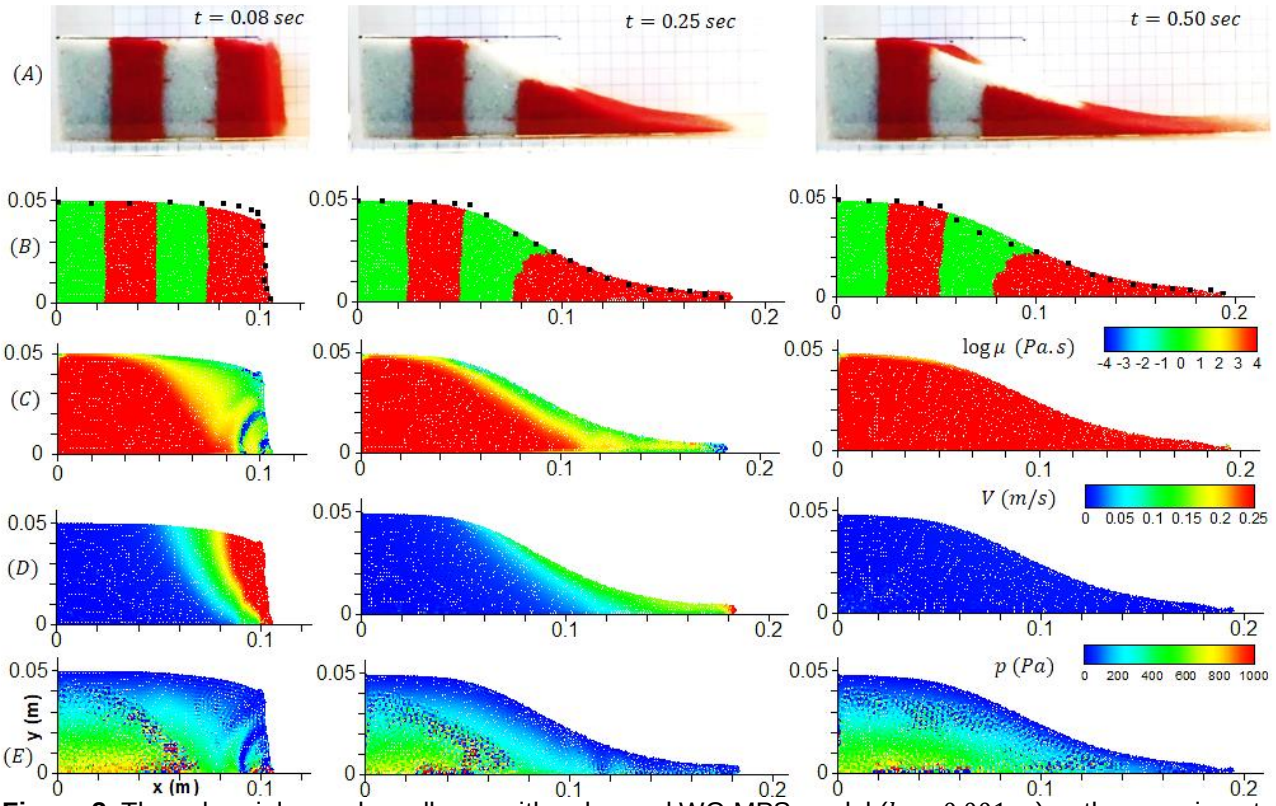

Figure 3. The subaerial granular collapse with enhanced WC-MPS model ($l_0 = 0.001\ m$) vs the experimental surface profiles (the black squares) (A) & (B), the viscosity (C), the velocity (D) and the pressure fields (E)

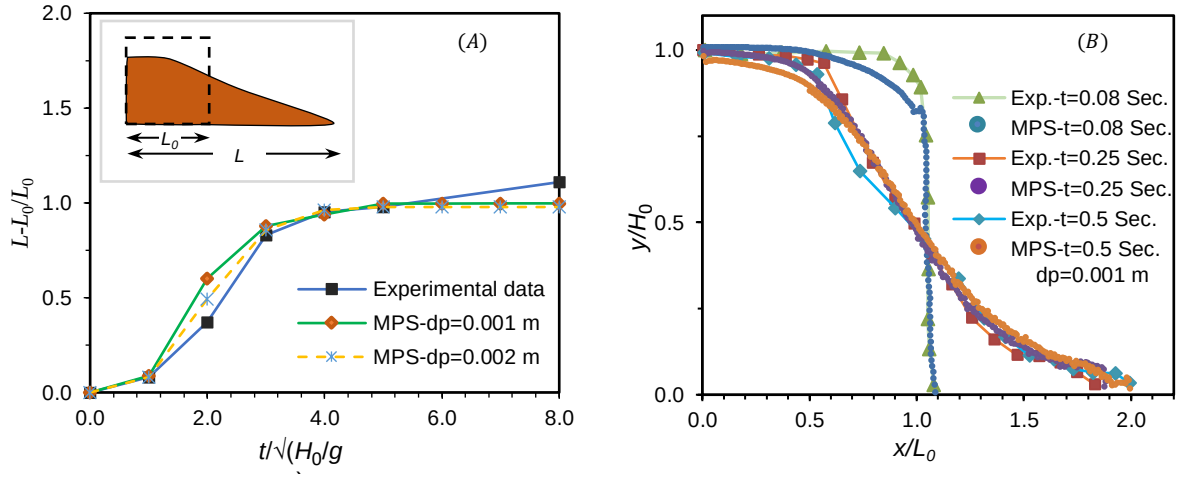

Figure 4. The runout distance ($l_0 = \mathrm{dp}$) (A) and the surface profiles (B) of the granular collapse vs the experimental results

Moreover, to validate the simulation results, we compare the flow surface profiles digitized from the experiments and the detected free surface particles of the numerical model for $t = 0.08, 0.25$ and 0.50 second in Figure 4B. With the non-dimensional runout distance of the granular collapse (L-L_0/L_0) and the time as $t/\sqrt{(H_0/g)}$, the numerical and experimental results are plotted in Figure 4A. The last sediment particle which is in contact with the bulk determines the front of the granular flow. Although the numerical model initially overestimates the runout distance (in both cases with $l_0 = 0.001$ and $0.002\ m$), the overall results of the numerical and experimental profiles are comparable in Figure 4.

The tensile instability (i.e. the fluid particles moving along the streamlines leading to the particle interpenetration) exists in the previous WC-MPS numerical results affecting the evolution of the granular collapse (Jafari Nodoushan et al., 2018). Here, by employing a conservative pressure gradient (Eq. [9]) and the enhancement algorithms (the OPS approach and the diffusive term (Eq. [15])) we aimed to surmount the tensile instability. In Figure 5, we show the pressure field and particles distribution of the numerical models with and without applying the diffusive term in the continuity equation and regularizing the particles with the particle shifting vector. Comparing Figure 5A & B illustrates the ability of the enhancement techniques in eliminating the tensile instability and representing a smooth pressure and particle distribution. Overall, the results obtained by the OPS regularization technique and the added diffusion term confirm that the proposed model eliminates the tensile instability and noisy pressure field to decrease the numerical and approximation errors.

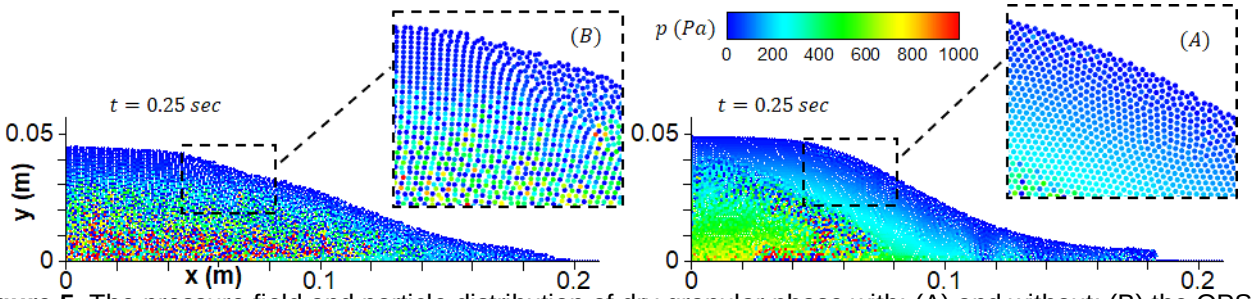

Figure 5. The pressure field and particle distribution of dry granular phase with; (A) and without; (B) the OPS technique and the diffusive term

3.2 Subaquatic granular collapse

We employ the validated model to simulate the submerged multiphase granular collapse as a two-dimensional problem with the initial particle size $l_0 = 0.002\ m$. As J. Nodoushan et al. (2018) noted, this problem belongs to the inertial regime of the immersed granular flows controlled by the drag force. The local *μ(I)* rheology updates the viscosity of the sediment particles, while the water particles have a constant viscosity set to $0.001\ Pa.s$ (the dynamic viscosity of water). Eq. [10] calculates the particles interactions due to the viscous shear stresses. The calculation time step is equal to 1×10^{-5} second with $c_0 = 10\ m/s$.

In Figure 6 we represent the time evolution of the subaquatic granular material (the green and blue colour particles) collapsing in ambient water (the yellow colour particles) simulated by our developed WC-MPS model. The granular surface profiles on the sidewalls of reservoir extracted from the experiments (the back squares) are plotted on the simulation outcomes at $t = 0.11$ and 0.54 second and the final stage of the granular collapse (Figure 6A). The discrepancy between the numerical model and experiments is the result of the three-dimensional effects of the submerged granular flow increasing the granular deposit close to the sidewalls (Figure 7) (i.e. the area of the granular material in the x-y plane adjacent to the sidewalls increases in the three-dimensional experiments). This effect was negligible in the dry case since the two-dimensional numerical model represented an accurate time evolution of the granular collapse vs the experimental data. With having the drag force acting on the granular particles in the submerged test case and without considering the sidewalls friction forces, the inconsistency between the granular deformation in the two-dimensional numerical model and the three-dimensional experiments becomes considerable. We should also note that the effects of the gate removal on the suspension of the nearby granules increase the discrepancy at the early time steps. However, the developed 2D numerical model simulates the flat top of the deposit more accurately in compare to the previous WC-MPS models.

The viscosity and velocity fields show the initial non-yielded zone of the submerged granular material as a trapezoidal shape at $t = 0.11$ (Figure 6B & C). After the granular material collapses, the stable condition occurs (i.e. where the viscosity reaches its maximum value and $V = 0$) at almost 1.29 second of simulation as the final stage. (The water particles are excluded from the Figure 6C & D to visible the granular flow properties only.)

Since the *μ(I)* rheology is a pressure dependent model, estimating an accurate pressure field plays an important role in simulating the mechanical behaviour of the granular flow. Employing the enhancement techniques in our WC-MPS model estimates a noise-free effective pressure field during the simulation of the collapse as illustrated in Figure 6D.

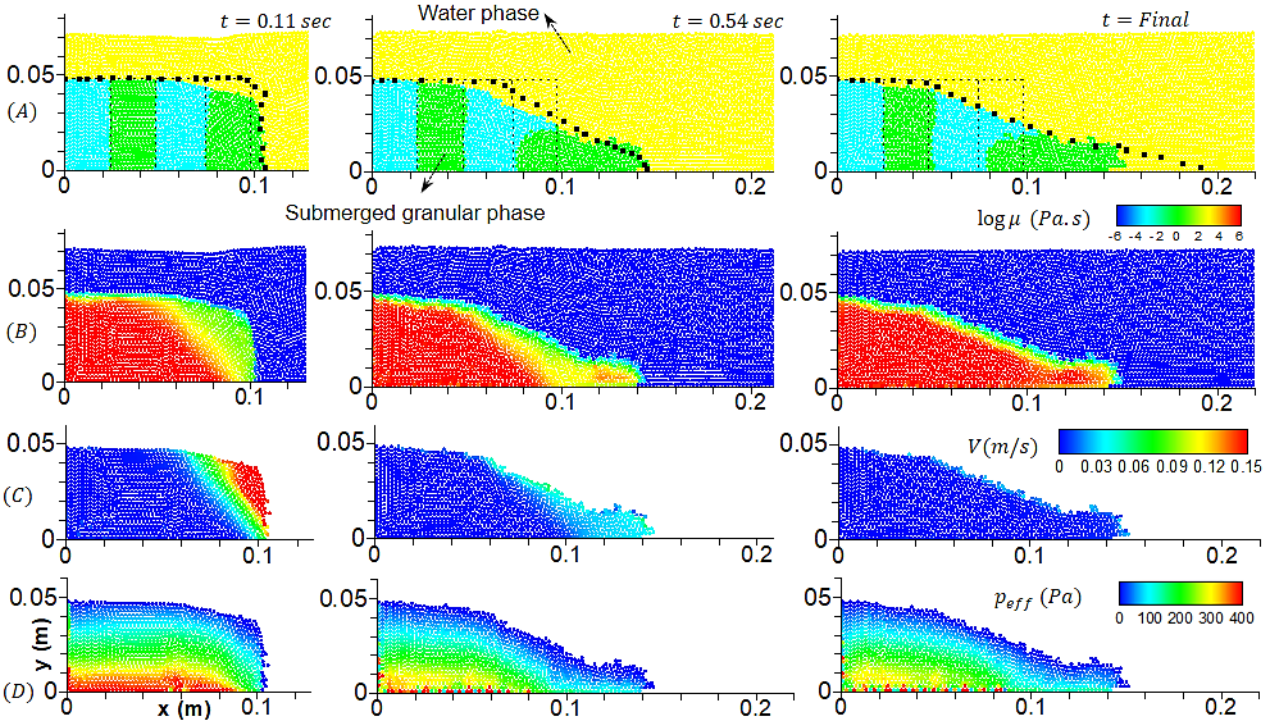

Figure 6. The subaquatic granular collapse with enhanced WC-MPS model ($l_0 = 0.002\ m$) vs the experimental surface profiles (the black squares) (A), the viscosity (C) and the effective pressure (D) fields

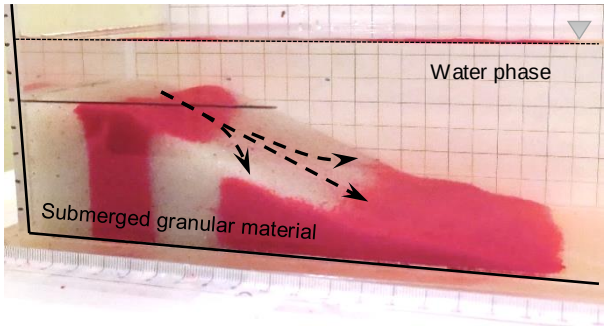

Figure 7. The final stage of the subaquatic granular collapse- The black arrows show the flow of granular material from the center toward the side and bottom walls in the three-dimensional configuration

In addition, we compare the overall deformation, the effective pressure and particle distributions within the granular phase for the models with and without the OPS method in Figure 8. We observe that to estimate accurate deformation of the granular material and surmount the tensile instability, applying the OPS algorithm is essential, although the diffusive term smooths the pressure field effectively (Figure 8A vs B). Without the regularizing the positions of the particles via the OPS method, they move along the streamlines causing an unrealistic deformation of the granular phase and effective pressure estimation.

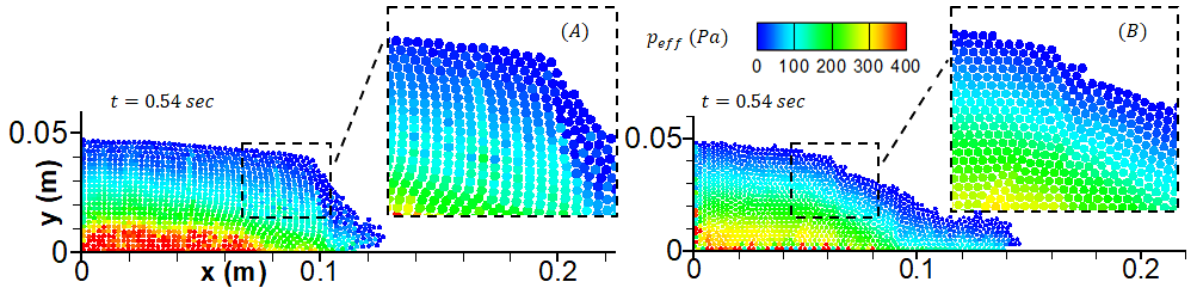

Figure 8. The effective pressure field and particle distribution of the submerged sediment phase with; (A) and without; (B) the OPS algorithm, the diffusion term is activated for both cases with $\delta = 0.2$

4 CONCLUSIONS

We represented a developed continuum-based WC-MPS model capable of simulating the mechanical behaviour of the dry and submerged granular collapses. As a multi-viscosity and multi-density system, the model

predicts the time evolution of the granular collapse using the regularized *μ(I)* rheology. The yield and flow behaviour of sediments were found to be sensitive to pressure fluctuations and tensile instability. Our proposed improvement techniques overcome the tensile instability and unphysical pressure fluctuations found to be effective in resolving this issue. To do so, we employed the particle shifting algorithm adopted with a conservative particle shifting vector in the context of the MPS method. Moreover, to reduce the pressure fluctuations and obtain a noise-free pressure field, we proposed a new diffusive term added to the continuity equation for calculating the particle number density. The good agreement between the experiments and the numerical outcomes; including the surface profiles and the runout distance of the subaerial granular collapse in different time steps, validated our proposed model. We extended the two-dimensional model to the subaquatic granular problem as a multiphase flow to simulate the collapse of the granular material within ambient water. We observed that the three-dimensional effects of the granular flow and the role of the sidewall's frictions affect the runout distance of the submerged granular collapse. Nevertheless, the flat top of the granular phase at the final stage is well predicted and the enhancement techniques eliminate the tensile instability over the domain. To include the three-dimensional effects of the granular collapse, we will develop the enhanced WC-MPS model to a three-dimensional model where the sidewall friction forces are directly considered. With these developments implemented, we aim to accomplish more accurate simulations of the multiphase sediment flows in the coastal and fluvial problems.

ACKNOWLEDGEMENTS

This research has been funded by Natural Sciences and Engineering Research Council of Canada (NSERC). Authors would like to thank Nvidia for supporting this research through their GPU Grant Program.

REFERENCES

Duan, G., Koshizuka, S., Yamaji, A., Chen, B., Li, X., & Tamai, T. (2018). An accurate and stable multiphase moving particle semi-implicit method based on a corrective matrix for all particle interaction models. *International Journal for Numerical Methods in Engineering,* 115(10), 1287-1314.

Forterre, Y., & Pouliquen, O. (2008). Flows of Dense Granular Media. *Annual Review of Fluid Mechanics,* 40(1), 1-24.

Jafari Nodoushan, E., Shakibaeinia, A., & Hosseini, K. (2018). A multiphase meshfree particle method for continuum-based modeling of dry and submerged granular flows. *Powder Technology,* 335, 258-274.

Jop, P. (2015). Rheological properties of dense granular flows. *Comptes Rendus Physique,* 16(1), 62-72.

Jop, P., Forterre, Y., & Pouliquen, O. (2006). A constitutive law for dense granular flows. *Nature,* 441, 727.

Khanpour, M., Zarrati, A.R., Kolahdoozan, M., Shakibaeinia, A., & Amirshahi, S.M. (2016). Mesh-free SPH modeling of sediment scouring and flushing. *Computers & Fluids,* 129, 67-78.

Khayyer, A., Gotoh, H., & Shimizu, Y. (2017). Comparative study on accuracy and conservation properties of two particle regularization schemes and proposal of an optimized particle shifting scheme in ISPH context. *Journal of Computational Physics,* 332, 236-256.

Koshizuka, S., & Oka, Y. (1996). Moving-particle semi-implicit method for fragmentation of incompressible fluid. *Nuclear science and engineering,* 123(3), 421-434.

Koshizuka, S., Shibata, K., Kondo, M., & Matsunaga, T. (2018). *Moving Particle Semi-implicit Method: A Meshfree Particle Method for Fluid Dynamics*. Academic Press, Book.

Lind, S.J., Xu, R., Stansby, P.K., & Rogers, B.D. (2012). Incompressible smoothed particle hydrodynamics for free-surface flows: A generalised diffusion-based algorithm for stability and validations for impulsive flows and propagating waves. *Journal of Computational Physics,* 231(4), 1499-1523.

Molteni, D., & Colagrossi, A. (2009). A simple procedure to improve the pressure evaluation in hydrodynamic context using the SPH. *Computer Physics Communications,* 180(6), 861-872.

Monaghan, J.J. (1992). Smoothed Particle Hydrodynamics. *Annual Review of Astronomy and Astrophysics,* 30, 543-574.

Monaghan, J.J., & Rafiee, A. (2013). A simple SPH algorithm for multi-fluid flow with high density ratios. *International journal for numerical methods in fluids,* 71(5), 537-561.

Shakibaeinia, A., & Jin, Y.-C. (2011). A mesh-free particle model for simulation of mobile-bed dam break. *Advances in Water Resources,* 34(6), 794-807.

Shakibaeinia, A., & Jin, Y.C. (2010). A weakly compressible MPS method for modeling of open-boundary free-surface flow. *International journal for numerical methods in fluids,* 63(10), 1208-1232.

Tajnesaie, M., Shakibaeinia, A., & Hosseini, K. (2018). Meshfree particle numerical modelling of sub-aerial and submerged landslides. *Computers & Fluids,* 172, 109-121.

Zubeldia, E.H., Fourtakas, G., Rogers, B.D., & Farias, M.M. (2018). Multi-phase SPH model for simulation of erosion and scouring by means of the shields and Drucker–Prager criteria. *Advances in Water Resources,* 117, 98-114.

